Available online at www.sciencedirect.com
SCIENCE DIRECT®
Dyes and Pigments 62 (2004) 199–212
DYES and PIGMENTS
www.elsevier.com/locate/dyepig

Structural and spectroscopic studies of iron (III) doped titania powders prepared by sol-gel synthesis and hydrothermal processing

R. Janes*, L.J. Knightley, C.J. Harding

Department of Chemistry, The Open University, Walton Hall, Milton Keynes, MK7 6AA, UK

Received 22 September 2003; received in revised form 30 November 2003; accepted 2 December 2003

Abstract

Iron-doped titania powders, of microfine dimensions and iron loadings of up to 5.64 wt.% were prepared by a sol-gel route. Gels, obtained by hydrolysis of titanium alkoxide in an aqueous solution of iron (II) chloride, were subjected to thermal treatment by heating in air or hydrothermal processing in an autoclave. The evolution of the crystalline component was determined by X-ray powder diffraction, and the local environment of the dopant was probed by electron spin resonance spectroscopy. Mössbauer spectroscopy was used to determine the oxidation state of the dopant. Over the iron-loading regime studied here, the anatase-rutile transition is inhibited at low dopant levels with respect to undoped titania. The effect becomes less pronounced as iron-loading is increased. Indeed the crystalline composition of the powders as a function of firing temperature is dependent not only on iron loading level but also on its dispersion within the titania matrix. This response is discussed in the context of the solution-based synthetic routes employed here.
© 2003 Elsevier Ltd. All rights reserved.

Keywords: Titania; Calcination; Hydrothermal; Doping; Spectrocopy

1. Introduction

Titanium dioxide is the most important white pigment in the paint, plastic and paper industries, largely due to its superior scattering properties, chemical stability and lack of toxicity [1]. A variety of titanium dioxide-based coloured pigments have also been produced by incorporating transition metal ions into the cationic sub-lattice. These include, brown pigments resulting from chromium and tungsten incorporation, and grey pigments resulting from the addition of iron and antimony [2]. Furthermore, transition metal ion dopants in TiO_2 have been shown to modify its photoactivity, which may help to offset the problem of 'chalking' (photooxidation of polymeric binders initiated by the pigment) that has long beset the coatings industry [3,4]. The influence of Fe (III) on the photoactivity of titania has been the particular focus of a study in which the structural and morphological response resulting from the dispersion of Fe^{3+} ions in titania, has been investigated [5].

* Corresponding author. Tel.: +44-020-7556-6149; fax: +44-020-7556-6196.
E-mail address: r.janes@open.ac.uk (R. Janes).

0143-7208/$ - see front matter © 2003 Elsevier Ltd. All rights reserved.
doi:10.1016/j.dyepig.2003.12.003

Bickley et al. suggested Fe^{3+} ions were well dispersed within the titania matrix at dopant levels up to 1 at.% iron. At higher levels, segregated hematite (α-Fe_2O_3) and pseudobrookite (Fe_2TiO_5) were also formed, the concentration of each being dependent on firing temperature [6]. Furthermore the presence of impurities or dopants in the titania lattice, has long been known to play a crucial role in determining the phase transformation kinetics [7].

Electron spin resonance (ESR) spectroscopy, which is a highly sensitive technique for the study of low levels of paramagnetic centres, has been used to study the iron-doped titania system, both for laboratory prepared samples and commercial pigments. Thorp and Eggleston [8] and Amorelli and co-workers [9] have used the technique to distinguish between surface and bulk Fe^{3+} ions in TiO_2, while De Biasi and co-workers used spectral linewidth as a gauge of the concentration of Fe^{3+} in rutile [10]. More recently, Egerton et al have used in-situ high temperature ESR as a means of calculating activation energies for diffusion of Fe^{3+} though the rutile lattice [11].

In the present work we examine the nature and extent of iron incorporation into the titania lattice by alkoxide-derived sol-gel synthesis and hydrothermal processing. It is well established that hydrolysis of alkoxides involves substitution (either nucleophilic or electrophilic depending on whether the reaction is base or acid catalysed respectively), followed by condensation reactions leading to the formation of oxo- and hydroxo-bridges yielding oligomeric oxoalkoxides. Gelation occurs when a so-called 'spanning cluster' is formed in the reaction vessel whereupon the enclosed solution remains entrapped [12]. Dried gels tend to be amorphous and some form of heat treatment is necessary to produce a crystalline product. Typically, samples are calcined in air, although treatment of dried gels in an autoclave under hydrothermal conditions affords the possibility of promoting crystallisation under milder conditions. This was first demonstrated in the context of the synthesis of nanoparticulate titania by Oguri et al [13]. There have been several reports of the use of sol-gel methods to synthesise iron-doped TiO_2 [14–17] but to the best of our knowledge hydrothermal processing has not yet been reported, although as noted by Braun, there is evidence in the patent literature of the use of hydrothermal methods to modify titania surfaces [1].

In this study we consider the composition of powders prepared by sol-gel and hydrothermal processing, particularly in the context of polymorphic phase transformation as a function of firing temperature and iron content. In this regard, an evaluation of the chemical nature of the dopant and its associated defect chemistry is important for understanding any observed modification to the properties of the host. To this end, ESR was employed as a diagnostic of dopant centres as a function of iron content and preparative method, and to provide a local probe of structural changes over the range of firing temperatures. Samples were also examined by Mössbauer spectroscopy, to establish the oxidation state and local environment of the iron.

2. Experimental

2.1. Sample preparation

All starting materials were obtained from the Aldrich Chemical Company and used without further purification. An aqueous solution of $FeCl_2.4H_2O$ was added dropwise to a solution of titanium isopropoxide in propan-2-ol with constant stirring, the concentrations being varied to produce the desired stoichiometry. The solution became progressively more viscous until a gel formed. This approach was developed from the recently published study by Lopez and co-workers [17] who prepared iron-doped sol-gel materials using an iron(II) precursor, and the earlier work of Rives et al., who found that the use of iron (II) rather that iron(III) yielded more uniform samples [18].

The gels were first dried in air at room temperature for 12 h, then calcined in air in a muffle furnace over a range of temperatures for the same length of time. Alternatively, the alkoxide derived gels were suspended in water and hydrothermally treated in a PTFE-lined autoclave at 220 °C under autogenous pressure for 4 h.

2.2. Sample characterisation

X-ray powder diffraction (XRD) patterns were obtained using a Seimens D5000 diffractometer using Cu-K_α radiation. Structural assignments were made with reference to the JCPDS powder diffraction file, and also using MAUD (Material Analysis Using Diffraction), a Java program developed by Lutterotti and co-workers [19]. Using the MAUD program, average particle sizes were also obtained from the Scherrer equation. In this context the term "particle" refers to a small single crystal, the size of which was determined by XRD. The quoted compositional information, is given as a percentage of the crystalline fraction, reproducibility being within ±5% of the reported results.

X-band (9.1 GHz) electron spin resonance spectra were measured using a Varian spectrometer with 100 kHz field modulation, and equipped with a nitrogen flow cryostat. All ESR spectra were recorded at −120 °C. Integrated spectra were obtained using the EPR-WARE program (Scientific Software Services, Illinois, USA) and fitting of simulated absorption spectra was carried out using Origin 7.0. ^{57}Fe Mössbauer spectra were recorded at 298 K using a microprocessor controlled instrument with a ca. 25mCi ^{57}Co/Rh source, calibration being carried out using a natural iron standard. Elemental analysis was carried out by inductively coupled plasma-atomic emission spectroscopy (ICP-AES) at MEDAC Ltd, Egham, Surrey, UK.

Table 1
Qualitative phase constitution of sol-gel derived TiO_2–Fe(x) powders calcined at various temperatures

x/%	T(calcination)/°C	Crystalline phases identified by XRD
0	120	–
0	200	Anatase and brookite (trace)
0	300	Anatase
0	500	Anatase, rutile
0	800	Rutile
0	1100	Rutile
0.13	120	–
0.13	200	–
0.13	300	Anatase (trace)
0.13	500	Anatase
0.13	800	Rutile
0.13	1100	Rutile
1.26	200	–
1.26	300	Anatase
1.26	500	Anatase
1.26	800	Rutile
1.26	1100	Rutile
2.85	120	–
2.85	200	–
2.85	300	Anatase and brookite (trace)
2.85	500	Anatase and brookite (trace)
2.85	800	Rutile and pseudobrookite
2.85	1100	Rutile and pseudobrookite
5.64	120	–
5.64	200	Anatase and brookite (trace)
5.64	300	Anatase and brookite(trace)
5.64	500	Anatase, rutile (trace) and brookite (trace)
5.64	800	Rutile and pseudobrookite
5.64	1100	Rutile and pseudobrookite

3. Results and discussion

3.1. Structural characterisation

Sol-gel derived materials of the following iron contents as determined by ICP-AES were prepared: 0.13, 1.26, 2.85 and 5.64 wt.%. Samples are referred to as TiO_2–Fe(x), where x is the iron content as wt.%. The qualitative phase composition derived from X-ray powder diffraction data for the materials is given in Table 1, and a representative series of patterns showing phase evolution as a function of temperature, is illustrated in Fig. 1. The onset of crystallisation occurred between 120–300 °C, with weak reflections from the anatase polymorph (present as a small fraction in a predominantly amorphous matrix) being detected. Phase transformation from anatase to rutile occurred between 500–800 °C and crystallisation to rutile is complete following firing at 1100 °C, with contributions from pseudobrookite Fe_2TiO_5 at the higher loading levels. The doped samples exhibit a colour gradation ranging from yellow at low dopant levels to dark brown at the highest iron loading, and the colour deepens as samples are fired at progressively higher temperatures.

The dried gels are amorphous for all compositions, which is in accord with the work of Petkov and coworkers who studied the short-range ordering in alkoxide derived pure titania gels using diffraction methods allied to simulation techniques [20]. The gels formed on hydrolysis were described in terms of short staggered chains of vertex and edge shared TiO_6 octahedral-like units and the mode of crystallisation was found to be dependent on the relative proportions of vertex- and edge-linked TiO_6 units within the amorphous material. It seems reasonable to suggest that Fe^{3+} will be integrated into these structures, although it is unclear as to its form. However as illustrated in Fig. 2 the dopant imposes a significant perturbation on the crystallisation behaviour. The XRD patterns for TiO_2–Fe(x) powders heated at 200 °C indicate partial crystallisation has occurred in the

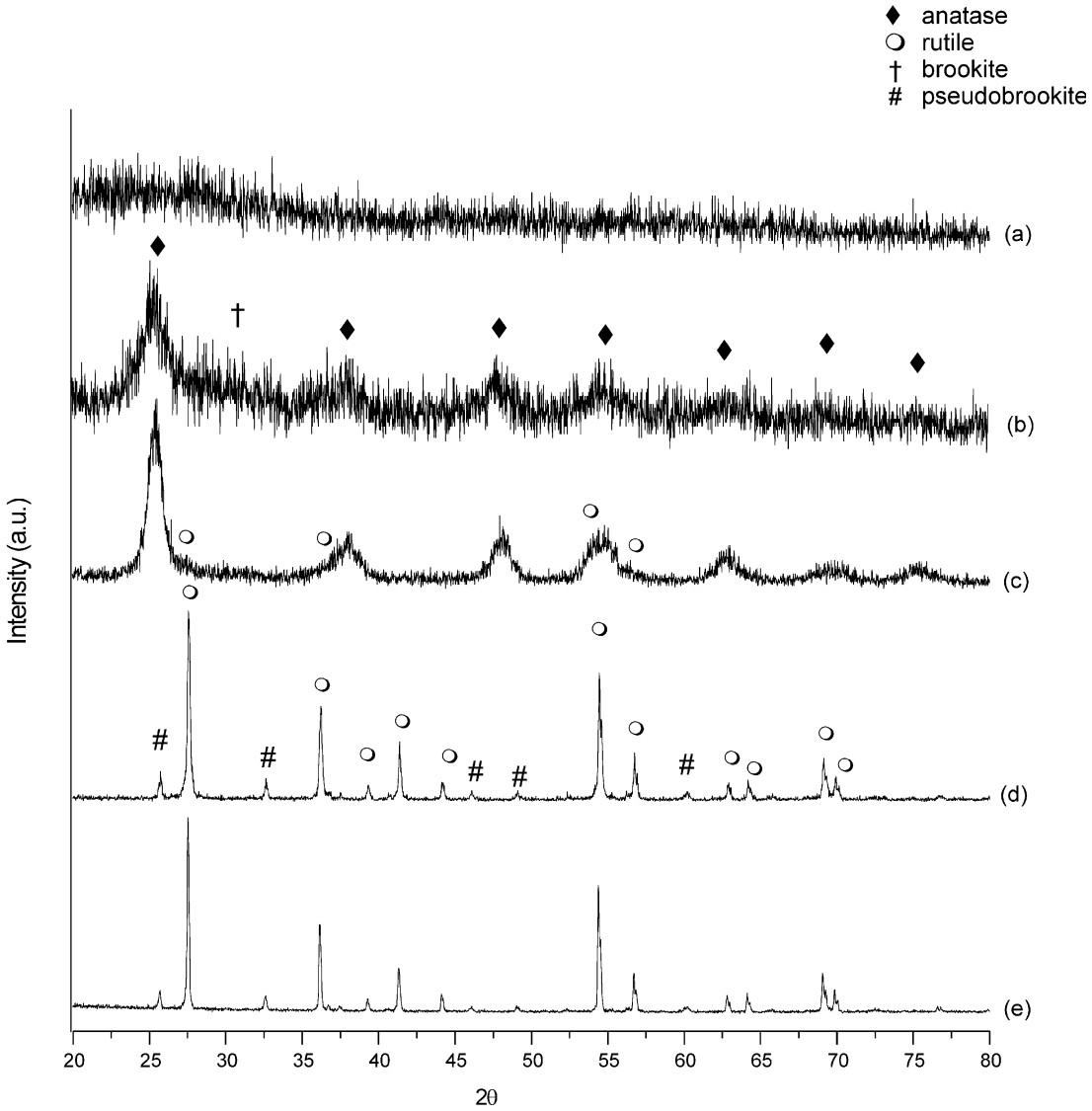

Fig. 1. XRD patterns obtained from the TiO_2–Fe (5.64) powders, calcined for 12 h at the following temperatures: (a) 120 °C, (b) 300 °C, (c) 500 °C, (d) 800 °C, (e) 1100 °C.

undoped material. By contrast at the lowest dopant level the sample remains amorphous by XRD criteria, although on increasing the iron content, more extensive crystallisation occurs. Here we interpret the undulations in the baseline of the patterns as indicative of incipient crystallisation. It is striking that at the highest iron concentration, clear evidence for crystallisation of anatase emerges. This is consistent with phase segregation of iron oxides or oxyhydroxides, which would pose less impediment to crystallisation at this level. Spectroscopic evidence for the formation of secondary inclusions is given in Section 3.2.

Following firing at 300 °C, crystalline anatase is formed in all samples (Table 1), with trace amounts of brookite being detected at higher iron loading. Given that the iron source used was iron (II) chloride, this response is in accord with the work of Pottier et al., who reported that a high chloride concentration, within an acidic medium promotes the crystallisation of brookite [21].

In the undoped sample, crystalline rutile was detected after firing at 500 °C. However, for the iron-loadings used in this work, it is clear the anatase-to-rutile transition is retarded, with no rutile being detected by XRD following firing at this temperature for an equivalent duration. The critical temperature range for phase transformation thus lies between 500 and 800 °C so, to gauge the effect of Fe^{3+} more closely, a detailed examination of the composition of powders fired over this range was carried out. Samples were calcined in 50 °C steps (for 12 h) and at each step the percentage of rutile in the crystalline fraction for each sample was determined [19]. As illustrated in Fig. 3, this clearly demonstrates inhibition of the rate of transformation to the rutile polymorph as Fe^{3+} is introduced. The effect is most marked at the lowest iron concentration, the extent of transformation becoming approximately equal to the undoped sample at the highest iron loading level. The reduction in rutile content for the TiO_2–Fe (5.64) sample above 700 °C is due to the contribution of pseudobrookite (Fe_2TiO_5) to the crystalline fraction, suggesting this phase is formed by reaction of the iron-doped rutile solid solution at this temperature.

The anatase to rutile transformation which arises by cleavage of two of the six Ti–O bonds in

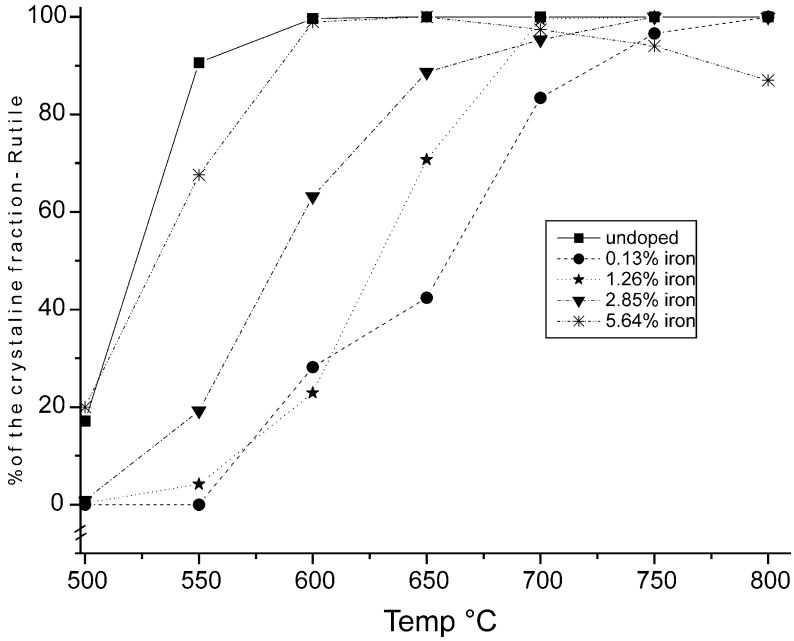

Fig. 2. XRD patterns obtained for the iron-doped titania powders calcined at 200 °C for 12 h: (a) undoped TiO_2, (b) TiO_2–Fe (0.13), (c) TiO_2–Fe (1.26), (d) TiO_2–Fe (2.85), (e) TiO_2–Fe (5.64).

the TiO_6 octahedra of anatase, occurs at a rate that is dependent on the nature (i.e. substitutional or interstitial incorporation) and extent of dopant incorporation into the titania lattice. It has previously been argued that oxygen vacancies can act as nucleation centres for the growth of rutile, and thus dopants which increase the concentration of oxygen vacancies, either in the bulk or on the surface, will accelerate the transition [22]. In this regard, substitutional incorporation of Fe^{3+} would generate oxygen vacancies on simple charge compensation grounds. Alternatively, interstitial occupancy, would reduce oxygen deficiency and, as argued by Arroyo et al., will stabilise the anatase phase [23]. We therefore infer that under the synthetic conditions employed here, Fe^{3+} preferentially enters interstitial positions in the anatase lattice, retarding the transformation rate. As the concentration is increased, lattice site occupancy is increased, which produces a concomitant enhancement in the transformation rate.

Calculated particle sizes for the TiO_2–Fe(x) powders are listed in Table 2. In contrast to anatase, there is some evidence for impeded grain growth of rutile. However, the effect is only observed in the $x = 1.26$ and 2.85 samples, implying that a minimum concentration of dopant is required, although we must qualify this statement

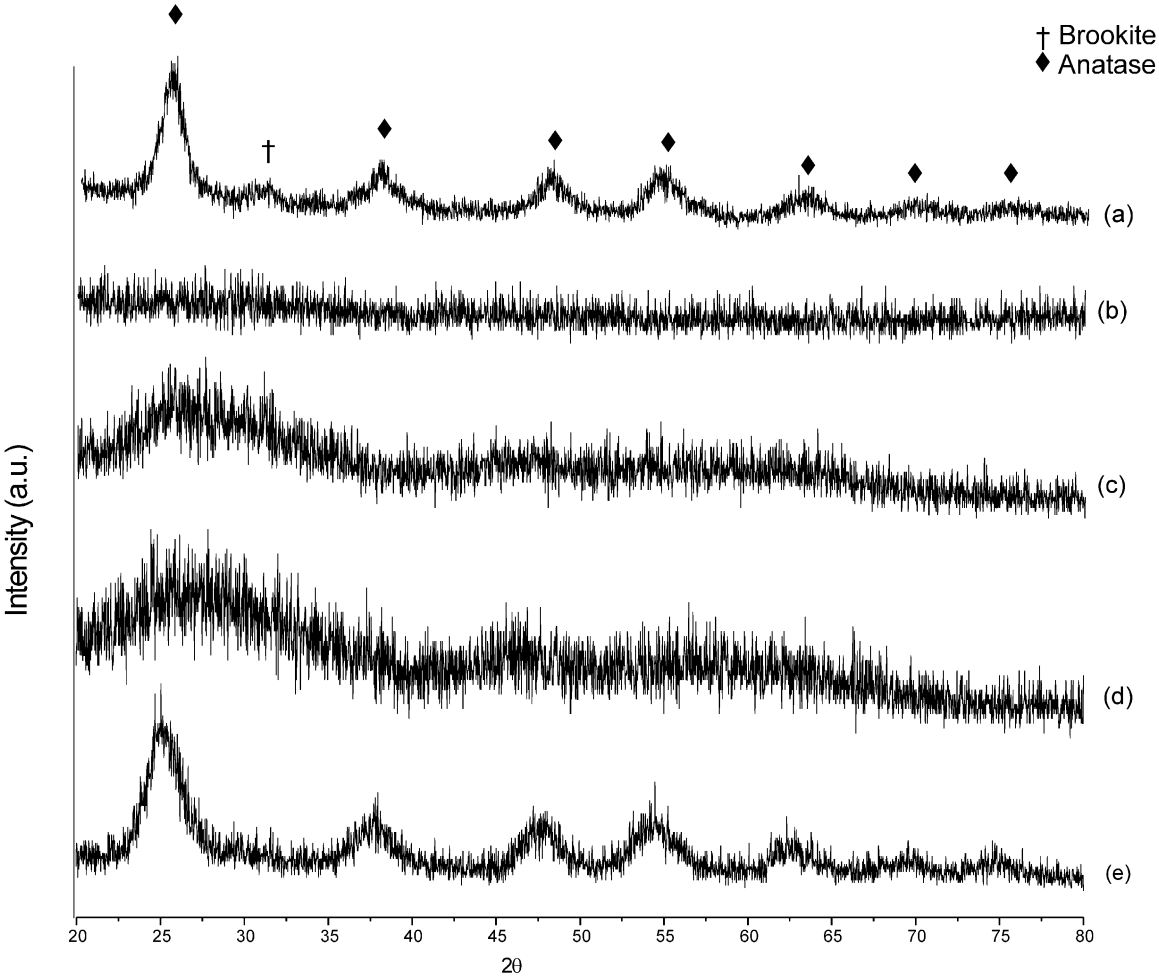

Fig. 3. Percentage of rutile in the crystalline fraction of TiO_2–Fe(x) powders heated between 500–800 °C for 12 h.

Table 2
Average titania particle sizes for TiO_2–Fe(x) powders prepared by calcination of alkoxide derived gels

x (wt.%)	T(calcination)/°C	Particle size (nm)[a]	
		Anatase	Rutile
0.00	300	13	
	500	17	24
	800		98
	1100		189
	300[b]		
	500	17	
	800		84
	1100		208
1.26	300	10	
	500	7	50
	800		44
	1100		50
2.85	300	9	
	500	11	
	800		66
	1100		87
5.64	300	8	
	500	10	
	800		114
	1100		228

[a] (±1 nm).
[b] Low intensity reflections prevented reliable calculation of particle size.

by noting that the linewidths of the XRD pattern indicate that at the highest iron loading level the particle size is unaffected.

The response reported in this work differs markedly from that observed for materials prepared by solid state reaction of anatase and iron oxides, where Fe_2O_3 has been shown to enhance the anatase to rutile transition [24]. Conversely, a recent study by Zhang and Reller demonstrate that the transition to rutile in sol-gel derived iron-doped titania occurs at a markedly higher temperature in the undoped material [16]. Furthermore, earlier studies have also suggested that excess iron in the titania lattice segregates as either haematite (α-Fe_2O_3) or pseudobrookite (Fe_2TiO_5). In this study, the former was never detected which, again, implies a high degree of molecular level mixing in the initial gel. In addition, it also seems reasonable to speculate that the presence of brookite at high iron loading may seed the formation of pseudo-brookite in preference to haematite, by providing a crystallographically similar surface.

3.2. Spectroscopic studies

To probe the oxidation state and local environment of the iron, these materials were examined by Mössbauer spectroscopy (from the point of view of instrumental sensitivity the TiO_2–Fe (5.64) samples were the most amenable to study). Representative spectra are shown in Fig. 4. The amorphous gel gave rise to a doublet having an isomer shift of 0.37 mm s^{-1} and quadrupole splitting of 0.69 mm s^{-1}. Following calcination at 800 °C, the doublet spectrum yielded an isomer shift of 0.38 mm s^{-1} and a quadrupole splitting of 0.75 mm s^{-1}. Both spectra are characteristic of Fe^{3+} in octahedral coordination [25], indicating this symmetry is prevalent in the amorphous material as well as being in accord with expectation for substitutional Fe^{3+} in rutile. We note that Fe^{2+} in the high-spin state would be expected to yield a spectrum with an isomer shift in the range +0.6 to +1.7 mm s^{-1} [25]. From a synthetic standpoint it is clear that Fe^{2+} has been oxidised in these materials, which is in contrast to a published study where the co-existence of Fe^{2+} and Fe^{3+} was demonstrated even following firing at 800 °C [17].

ESR spectra from materials produced by the sol gel route, differ markedly from those reported previously from materials prepared by the impregnation, or solid state methods [8–11]. These are illustrated in Fig. 5–9, spectra shown for each firing temperature and iron-loading. These differences, we suggest, are further consequence of differences in the extent of incorporation of iron into the titania lattice, which are expected to be optimised by the molecular level mixing implicit in the sol-gel route. Clear similarities exist between the spectra of amorphous samples and those containing crystalline anatase fractions within an amorphous matrix. Two major resonances were detected; a signal at $g = 4.3$ (with a shoulder extending to lower field) and a signal at $g = 2.00$. The former is characteristic of high-spin Fe^{3+} in a

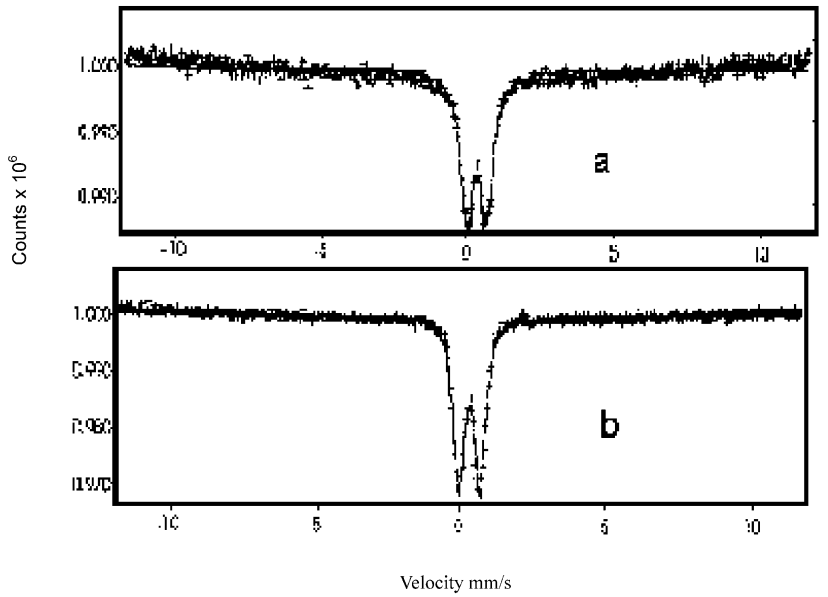

Fig. 4. Mossbauer spectra obtained from TiO_2–Fe (5.64) (A) dried gel, (B) following calcining at 800 °C for 12 h.

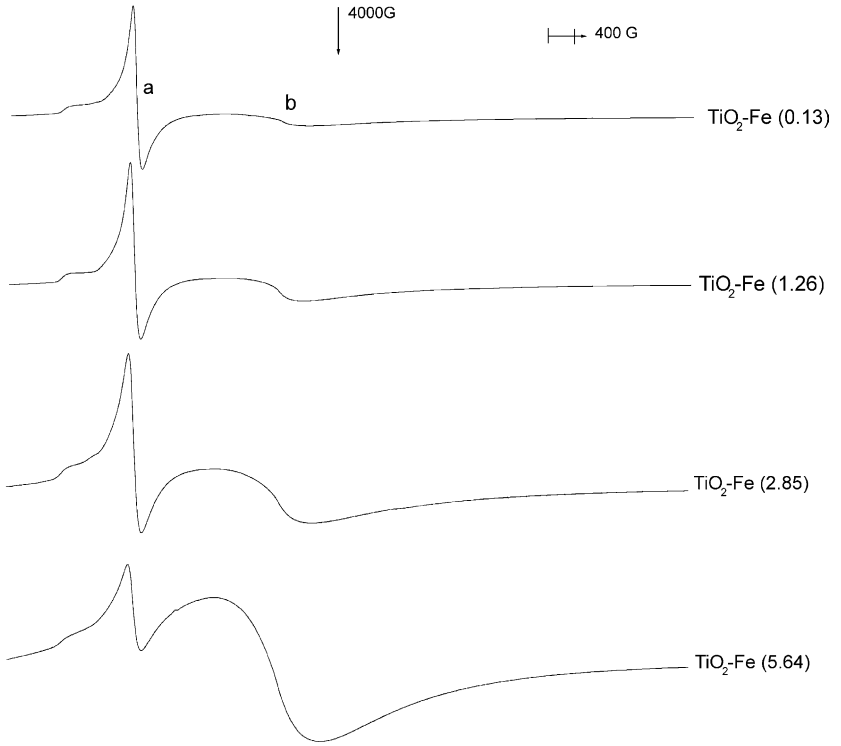

Fig. 5. First derivative X-band ESR spectra for TiO_2–Fe(x) dried gels, where a: $g = 4.3$ and b: $g = 2.0$.

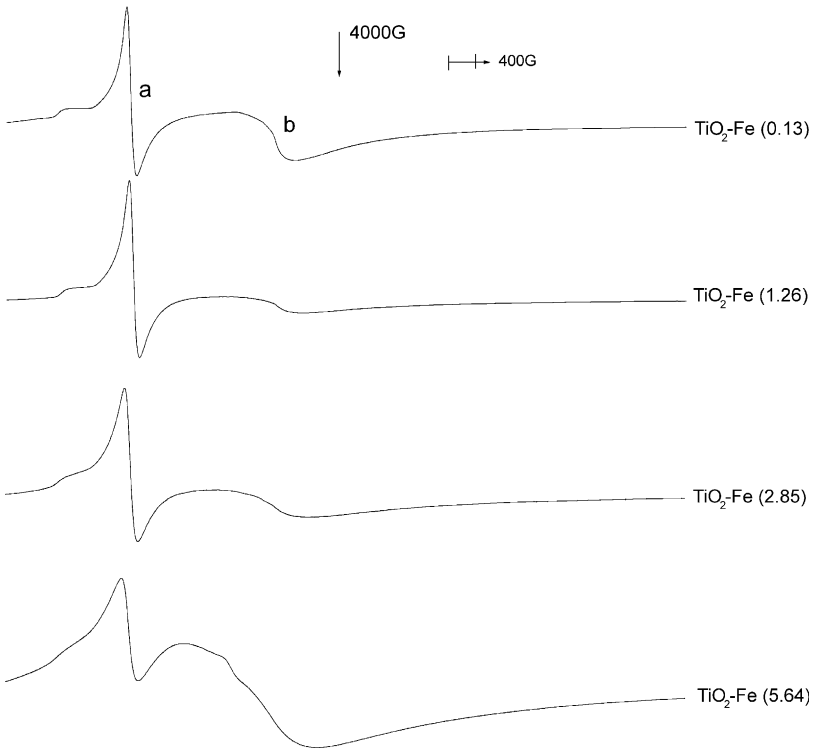

Fig. 6. First derivative X-band ESR spectra for TiO_2–Fe(x) powders, calcined at 120 °C for 12 h, where a: $g = 4.3$ and b: $g = 2.0$.

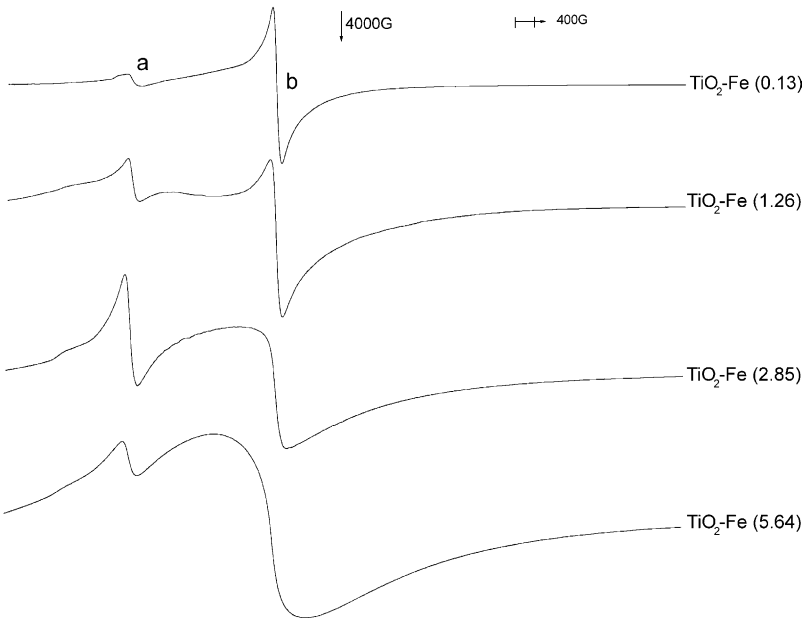

Fig. 7. First derivative X-band ESR spectra for TiO_2–Fe(x) powders, calcined at 300 °C for 12 h, where a: $g = 4.3$ and b: $g = 2.0$.

rhombic environment and the latter has been assigned to Fe^{3+} in sites of axial symmetry. It is evident that these centres persist from the amorphous through to the crystalline state. In addition, a feature at $g = 2.00$ grew as the firing temperature was increased to 500 °C. On consideration of conjoint XRD data (Table 1), the ESR spectra obtained following firing at this temperature may be assigned to Fe^{3+} substituted anatase.

The signal at $g = 4.3$ diminishes markedly as the firing temperature is increased to 500 °C. Previous ESR studies on rutile samples impregnated with an aqueous Fe^{3+} solution have assigned a signal at $g = 4.3$ to surface iron which diffused into the bulk on heat treatment. However, in this work we start with an amorphous gel into which the dopant is intimately incorporated, and which develops into a regular assembly on thermal treatment. Thus the $g = 4.3$ signal detected from our samples arises from Fe^{3+} in a rhombic environment within these amorphous materials. However, the possibility of iron diffusion towards the surface on gel formation cannot be discounted. A further feature of the spectra of these materials, is the presence of a very broad underlying resonance in the $g = 2.00$ region. This component becomes more obvious as the iron content is increased. Its presence was verified by integration of the spectrum of the TiO_2–Fe(5.64) sample fired at 500 °C over the $g \sim 2$ region. The integrated spectrum comprises a broad absorption with a sharp centre, which may be simulated precisely by the superposition of two Lorentzian functions, consistent with a non-saturating ESR transition. We conclude that this feature results from the overlap of a major broad component (1680 G with an 98% weighting) and a minor narrow component (144 G). At this point it is not possible unequivocally to assign this broad component to a particular species, but we speculate that it arises from an iron oxide or iron

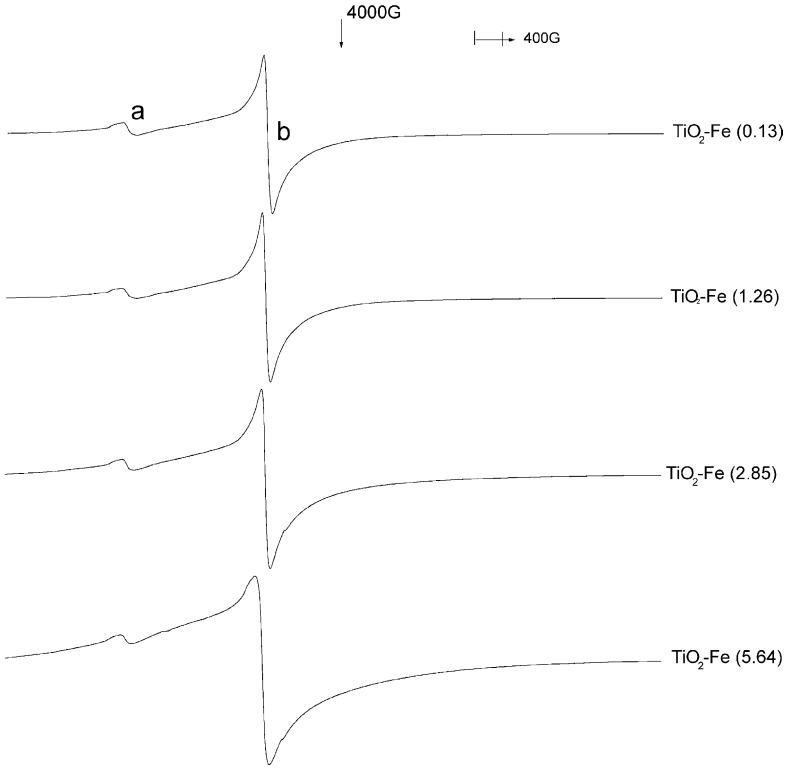

Fig. 8. First derivative X-band ESR spectra for TiO_2–Fe(x) powders, calcined at 500 °C for 12 h, where a: $g = 4.3$ and b: $g = 2.0$.

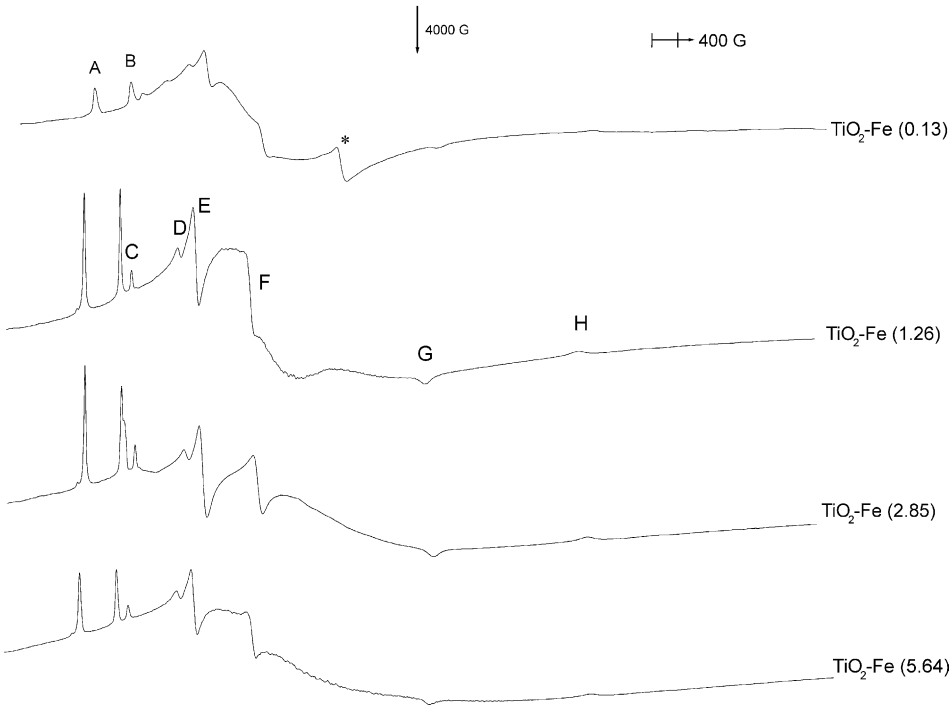

Fig. 9. First derivative X-band ESR spectra for TiO_2–Fe(x) powders, calcined at 800 °C for 12 h.

oxy-hydroxide phase present at levels below the XRD detection limits. For example we note that the ESR spectrum of hematite (α-Fe_2O_3) has a linewidth of ca. 2000 G [26].

Following annealing to 800 °C, a multi-component spectra was detected (Fig. 9), the g-values for each species are listed in Table 3. The spectra are labelled in accord with published data for the Fe^{3+} doped rutile system, prepared by solid-state reaction or impregnation[8,11]. Egerton and co-workers have previously assigned these signals to substitutional Fe^{3+} in sites of tetragonal symmetry [11]. However, closer consideration of our data reveals the appearance of new features, having $g = 5.0$, 3.7, and 1.1 in addition to those previously reported. For high-spin Fe^{3+}, Aasa has carried out a detailed theoretical treatment of the powder ESR spectra [27]. Line positions were defined in terms of the ratio of zero-field parameters D and E. Clearly these additional signals arise from dopants in crystallographic discrete sites, not formed in materials produced by solid-state or impregnation routes, and are a further consequence of mixing at the molecular level in the precursor.

Table 3
Measured g-values for iron doped titania powders following heat treatment at 800 °C

Resonance	g-value
A	8.2
B	5.7
C	5.0
D	3.7
E	3.3
F	2.6
G	1.5
H	1.1
*	2.0 *($x = 0.13$ sample only)*

The $g = 2.0$ signal is still evident in the spectra from TiO_2–Fe (0.13) fired to 800 °C, but is not detected at higher substitutional levels. From the 1.26, 2.85 and 5.64 wt.% samples, there is no evidence for the $g = 2.00$ signal following heat treatment at this temperature. Refinement of the XRD

patterns by the MAUD programme does, indeed, reveal evidence of low-level anatase in the crystalline fraction of this sample, which further supports the assignment of this resonance to Fe^{3+} substituted in an anatase host. The spectra of the iron doped materials fired at 800 °C are also characterised by a broad underlying resonance extending to high field. Although no equivocal assignment is possible, we may speculate that the presence of secondary iron oxides, or pseudobrookite may be the origin of this signal.

3.3. Hydrothermal treatment of alkoxide derived gels

As an alternative to calcination in air, iron-doped alkoxide gels were also heated as a slurry in water in an autoclave. Fig. 10 shows, XRD patterns for the resulting samples over the complete iron concentration range. These iron-doped alkoxide gels yielded crystalline anatase for all compositions. Trace amounts of brookite are also evident, an observation previously reported following

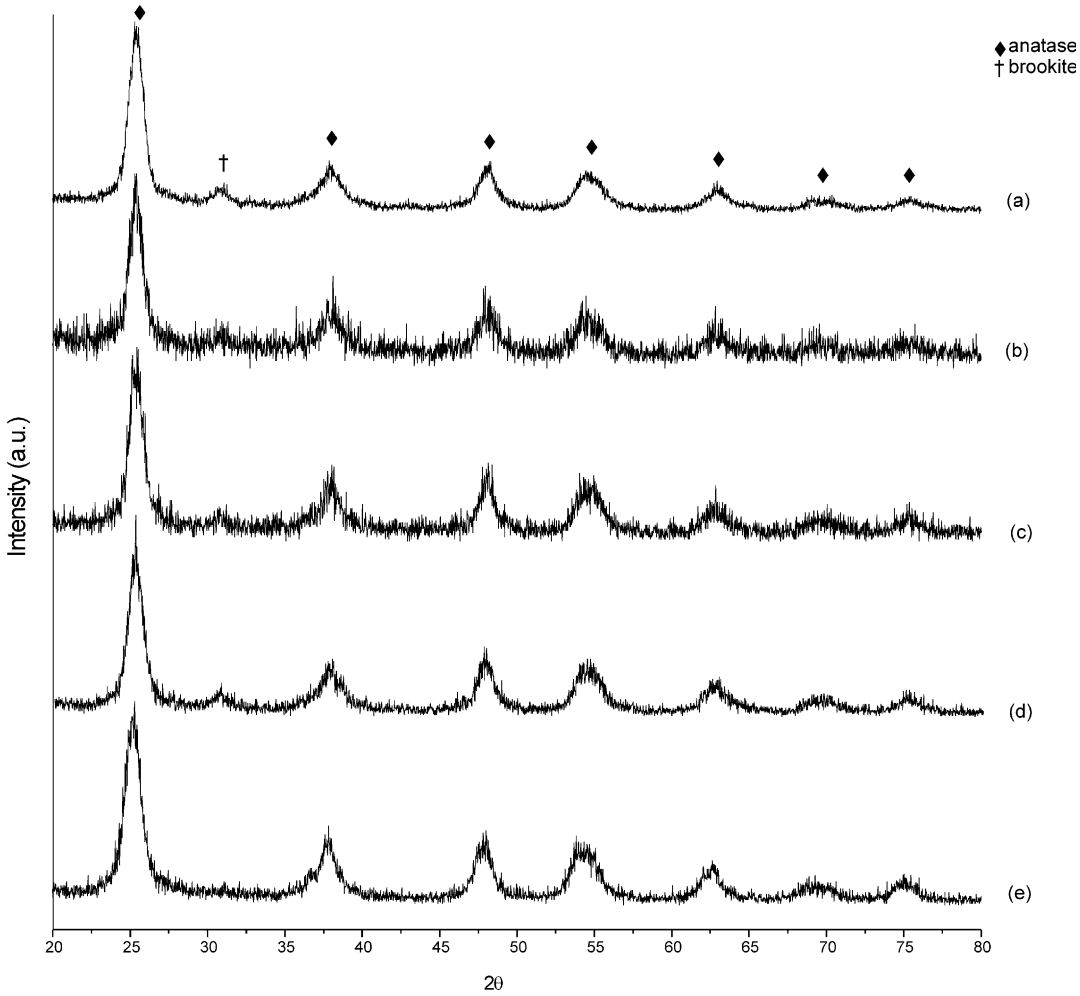

Fig. 10. XRD patterns for TiO_2–Fe(x) powders produced by treatment of alkoxide derived gels in an autoclave. (a) Undoped, (b) TiO_2–Fe (0.13), (c) TiO_2–Fe (1.26), (d) TiO_2–Fe (2.85), (e) TiO_2–Fe (5.64).

hydrothermal treatment of titanium alkoxide-derived gels following addition of excess chloride ions [28]. Calculated particle sizes for anatase ranged from 6–10 nm over the series. We also note a decrease in the signal-to-noise ratio on the introduction of the dopant. This series clearly parallels our observations for the calcined materials where crystallisation was impeded on addition of Fe^{3+} ions although increasing crystallinity was observed (as gauged by decreasing signal-to-noise ratio) on increasing the dopant level, presumably resulting from segregation of an iron-rich secondary phase.

The ESR spectra of the hydrothermally treated samples (Fig. 11) comprised two well defined components. The $g = 4.3$ signal assigned to surface Fe^{3+} ions and a resonance at $g = 2.0$ consistent with anatase. The latter broadened considerably and became highly asymmetric as the Fe^{3+} concentration increased. Again, as for the calcined samples, we suggest this is indicative of the formation of secondary iron oxide or oxy-hydroxide inclusions.

4. Conclusions

Iron doped titania has been prepared by heat treatment of amorphous gels formed from hydrolysis reactions of alkoxides, either in air or under hydrothermal conditions. XRD patterns indicated the dopant had a profound effect on both crystallisation from the gel and phase evolution on heating, and marked differences with published data from samples prepared by solid state synthesis or impregnation, were attributed to a greater degree of mixing in the precursor. In particular the anatase to rutile transition was retarded on addition of iron, although at the highest loading level the extent of transformation was approximately equal to the undoped material. Segregation of an unidentified secondary iron-rich phase was inferred in

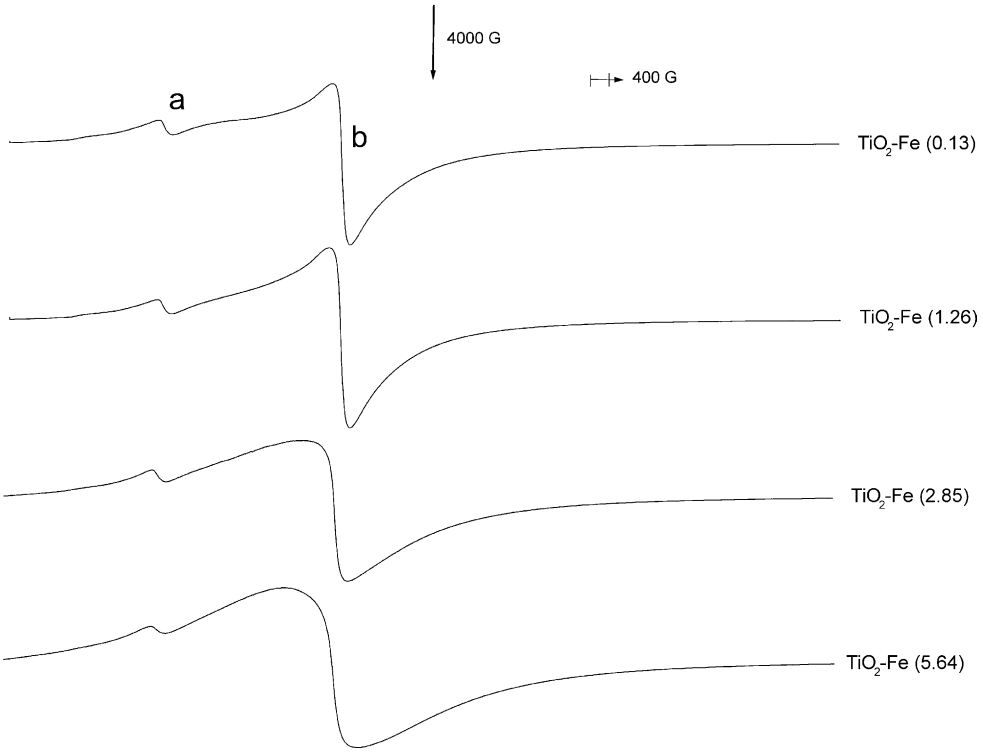

Fig. 11. First derivative X-band ESR spectra for TiO_2–Fe(x) samples following hydrothermal treatment, where a: $g = 4.3$ and b: $g = 2.0$.

samples containing the highest Fe^{3+} content. ESR spectroscopy yielded information regarding the nature and extent of dopant incorporation and corroborated the presence of iron-rich secondary phases at high iron loadings.

Acknowledgements

The authors would like to thank Mr G Oates for technical assistance, Professor FJ Berry for many helpful discussions, and the Open University for financial support.

References

[1] Braun JH. White pigments. Federation of Societies for Coatings Technology; 1995.
[2] Buxbaum G. Industrial inorganic pigments. Wiley-VCH; 1998.
[3] Allen NS. Photofading and light stability of dyed and pigmented polymers. Polym Degrad Stab 1994;44:357–74.
[4] Janes R, Edge M, Robinson J, Allen NS. Microwave photodielectric and photoconductivity studies of commercial titanium dioxide pigments: the influence of transition metal dopants. J Mater Sci 1998;33:3031–6.
[5] Litter MI, Navio JA. Photocatalytic properties of iron-doped titania semiconductors. J Photochem Photobiol A Chemistry 1996;98:171–81.
[6] Bickley RI, Lees JS, Tilley RJD, Palmisano L, Schiavello M. Characterisation of iron/titanium oxide photocatalysts. Part 1- structural and magnetic studies. J Chem Soc Faraday Trans 1992;88:377–83.
[7] Shannon RD, Pask JA. Kinetics of the anatase-rutile transformation. J Am Ceram Soc 1965;48:391–8.
[8] Thorp JS, Eggleston HS. Rhombic symmetry sites in Fe/TiO_2 powders. J Mater Sci Letts 1985;4:1140–2.
[9] Amorelli A, Evans JC, Rowlands CC, Egerton TA. An ESR study of rutile and anatase titanium dioxide polycrystalline powders treated with transition metal ions. J Chem Soc Faraday Trans 1 1987;83:3541–8.
[10] De Biasi RS, Fernandes AAR, Grillo MLN. Measurement of small concentrations of chromium and iron in rutile using electron spin resonance. J Am Ceram Soc 1993;76:223–5.
[11] Egerton TA, Harris E, Lawson EJ, Mile B, Rowlands CC. An EPR study of diffusion of iron into rutile. Phys Chem Chem Phys 2001;3:497–504.
[12] Wright JD, Sommerdijk NAJM. Sol-gel materials chemistry and applications. Gordon and Breach Science Publishers; 2001.
[13] Oguri Y, Riman RE, Bowen HK. Processing of anatase prepared from hydrothermally treated alkoxy-derived hydrous titania. J Mater Sci 1988;23:2897–904.
[14] Wang C, Bahnemann DW, Dohrmann JK. A novel preparation of iron-doped TiO_2 nanoparticles with enhanced photocatalytic activity. Chem Commun 2000:1539–40.
[15] Wang JA, Limas-Ballesteros R, Lopez T, Moreno A, Gomez R, Novaro O, et al. Quantitative determination of titanium lattice defects and solid-state reaction mechanism in iron-doped TiO_2 photocatalysts. J Phys Chem B 2001;105:9692–8.
[16] Zhang YH, Reller A. Nanocrystalline iron-doped mesoporous titania and its phase transition. J Mater Chem 2001;11:2537–41.
[17] Lopez T, Moreno JA, Gomez R, Bokhimi X, Wang JA, Yee-Madeira H, et al. Characterisation of iron-doped titania sol-gel materials. J Mater Chem 2002;12:714–8.
[18] Rives AB, Kulkarni TS, Schwaner AL. N_2 and H_2O adsorption on combinations of TiO_2 and Fe_2O_3. Langmuir 1993;9:192–6.
[19] Lutterotti L, Mattheis S, Wenk HR. MAUD (Material Analysis Using Diffraction): a user friendly Java program for Rietveld texture analysis. In ICOTOM (International Conference on the Textures of Materials) 12, Montreal, 1999.
[20] Petkov V, Holzhuter G, Troge U, Gerber Th, Himmel A. Atomic scale structure of amorphous TiO_2 by electron, X-ray diffraction and reverse Monte Carlo simulations. J Non-Cryst Solids 1998;231:17–30.
[21] Pottier A, Chaneac C, Tronc E, Mazerolles L, Jolivet JP. Synthesis of brookite TiO_2 nanoparticles by thermolysis of $TiCl_4$ in strongly acidic aqueous media. J Mater Chem 2001;11:1116–21.
[22] Shannon RD, Pask JA. Kinetics of the anatase-rutile transformation. J Am Ceram Soc 1965;48:391–8.
[23] Arroyo R, Corgoba G, Padilla J, Lara VH. Influence of manganese ions on the anatase-rutile phase transition of TiO_2 prepared by the sol-gel process. Mater Letts 2002;54:397–402.
[24] Gennari FC, Pasquevich DM. Kinetics of the anatase-rutile transformation in TiO_2 in the presence of Fe_2O_3. J Mater Sci 1998;33:1571–8.
[25] Dixon DPE, Berry FJ. Mössbauer Spectroscopy. Cambridge University Press; 1986.
[26] Guskos N, Papadopoulos GJ, Likodimos V, Patapis S, Yarmis D, Przepiera A, et al. Photoacoustic, EPR and electrical conductivity investigations of three synthetic mineral pigments: haematite, goethite and magnetite. Mater Res Bull 2002;37:1051–161.
[27] Aasa R. Powder line shapes in the electron paramagnetic resonance spectra of high spin ferric complexes. J Chem Phys 1970;52:3919–30.
[28] Wang CC, Ying JY. Sol-gel synthesis and hydrothermal processing of anatase and rutile titania nanocrystals. Chem Mater 1999;11:3113–6.